RAFT Dispersion Polymerization in Silicone Oil

Matthew J. Rymaruk,[a] Saul J. Hunter,[a] Cate T. O'Brien,[a] Steven L. Brown,[b] Clive N. Williams,[b] and Steven P. Armes,[a,]*

a. Dainton Building, Department of Chemistry, University of Sheffield, Brook Hill, Sheffield, South Yorkshire, S3 7HF, UK.

b. Scott Bader Company Ltd, Wollaston, Wellingborough, Northamptonshire, NN29 7RL, UK.

*s.p.armes@sheffield.ac.uk

For Table of Contents use only

RAFT dispersion polymerization in silicone oil (D5)

Increasing PDMA DP (x)

Spheres x = 49 — 100 nm

Worms x = 100 — 400 nm

Vesicles x = 186 — 500 nm

ABSTRACT. A near-monodisperse monohydroxy-terminated polydimethylsiloxane (PDMS; mean degree of polymerization = 66) was esterified using a carboxylic acid-functionalized trithiocarbonate to yield a $PDMS_{66}$ precursor with a mean degree of functionality of 92 ± 5 % as determined by ^1H NMR spectroscopy. This $PDMS_{66}$ precursor was then chain-extended in turn using nine different methacrylic monomers in a low-viscosity silicone oil (decamethylcyclopentasiloxane, D5). Depending on the monomer type, such PISA syntheses proceeded via either RAFT dispersion polymerization or RAFT emulsion polymerization. In each case the target DP of the core-forming block was fixed at 200 and the copolymer concentration was 25 % w/w. Transmission electron microscopy studies indicated that kinetically-trapped spheres were obtained in almost all cases. The only exception was 2-(dimethylamino)ethyl methacrylate (DMA), which enabled access to spheres, worm or vesicles. This striking difference is attributed to the relatively low glass transition temperature for this latter block. A phase diagram was constructed for a series of $PDMS_{66}$-$PDMA_x$ nano-objects by systematically increasing the PDMA target DP from 20 to 220 and varying the copolymer concentration between 10 and 30 % w/w. Higher copolymer concentrations were required to access a pure worm phase, whereas only spheres, vesicles or mixed phases were accessible at lower copolymer concentrations. Gel permeation chromatography studies indicated a linear evolution of number-average molecular weight (M_n) with PDMA DP while dispersities remained below 1.39, suggesting relatively well-controlled RAFT polymerizations. Small angle x-ray scattering (SAXS) was used to characterize selected examples of spheres, worms and vesicles. $PDMS_{66}$-$PDMA_{100-112}$ worms synthesized at 25 - 30 % w/w formed free-standing gels at 20 °C. Oscillatory rheology studies performed on a 30 % w/w PDMS-$PDMA_{105}$ worm dispersion indicated a storage modulus (gel strength) of 1057 Pa and a critical gelation concentration (CGC) of 12 % w/w. Finally, $PDMS_{66}$-$PDMA_x$ worms could also be prepared in *n*-dodecane, hexamethyldisiloxane or octamethylcyclosiloxane. Rotational rheometry studies indicate that such worms are efficient viscosity modifiers for these non-polar oils.

Introduction

It has been well-known for more than fifty years that AB diblock copolymers undergo self-assembly when placed in a selective solvent for either block.[1–3] This spontaneous process has been widely used to access various copolymer morphologies, including spheres, worms (or rods) and vesicles.[4–9] Traditionally, the diblock copolymer is first prepared in a good solvent for both blocks. Self-assembly of the molecularly-dissolved copolymer chains is then induced by gradually worsening the solvency for one of the blocks. However, this processing route is normally limited to rather low copolymer concentrations (typically less than 1.0 % w/w).[10,11]

Over the past decade or so, polymerization-induced self-assembly (PISA) has emerged as a robust strategy for the convenient synthesis of a range of diblock copolymer nanoparticles directly in the form of concentrated dispersions.[12–15] Typically, a controlled radical polymerization technique such as reversible addition-fragmentation chain transfer (RAFT) polymerization[16–19] is used to prepare the precursor block, which is dissolved in a good solvent. The second block is selected such that it is insoluble in this solvent. Thus, as the second-stage polymerization proceeds, the growing second block eventually becomes insoluble when it reaches a certain critical degree of polymerization (DP), which drives *in situ* self-assembly to form sterically-stabilized nanoparticles. Such PISA syntheses eliminate the requirement for any post-polymerization processing steps and can be conducted at up to 50 % w/w solids.[20]

Recently, we reported the conversion of a monohydroxy-capped polydimethylsiloxane (PDMS) precursor into a macromolecular RAFT chain transfer agent and studied its subsequent chain extension with benzyl methacrylate (BzMA) in *n*-heptane.[21] Systematic variation of (i) the target degree of polymerization for the core-forming poly(benzyl methacrylate) (PBzMA) block and (ii) the copolymer concentration selected for such PISA syntheses enabled the synthesis of pure spheres, worms or vesicles via RAFT dispersion polymerization. The single example of PDMS$_{66}$-PBzMA$_{80}$ diblock copolymer

worms identified in this prior study formed a free-standing gel at room temperature, most likely owing to multiple inter-worm contacts.

PISA syntheses have been performed in various solvents, including water,[22–27] alcohol,[28–33] ionic liquids,[34] chloroform,[35,36] and various non-polar solvents, including n-alkanes,[33,37,38] supercritical CO_2,[39,40] mineral oil and poly(α-olefins).[20] However, as far as we are aware, there have been no reports of PISA syntheses being conducted in silicone oil. In principle, the $PDMS_{66}$ macro-CTA described above should be a suitable stabilizer block for such PISA syntheses; in contrast, most (meth)acrylic copolymers are insoluble in silicone oil.

Silicones comprise a unique class of liquid polymers, oligomers or small molecules whose highly flexible backbones are composed of inorganic Si-O-Si bonds. The most common silicone oil is polydimethylsiloxane (PDMS). Silicone oils are non-toxic, chemically inert and non-flammable.[41] They are used as anti-foaming agents,[42] in medical devices,[41] as hydraulic fluids[43] and in various cosmetic formulations.[44] In addition, cyclic silicones such as decamethylcyclopentasiloxane (D5) or dodecamethylcyclohexasiloxane (D6) exhibit relatively low viscosity and high volatility, enabling their widespread use as lubricious carrier fluids in personal care products such as deodorants and antiperspirants.[44,45]

In the present study, we have converted a commercially available monohydroxy-functional $PDMS_{66}$ precursor (where the subscript denotes its mean degree of polymerization) into a trithiocarbonate-based macromolecular chain transfer agent ($PDMS_{66}$-TTC macro-CTA) for the RAFT dispersion polymerization of a range of methacrylic monomers in D5 silicone oil. Perhaps surprisingly, only one of these monomers allowed access to the full range of copolymer morphologies. A phase diagram was constructed to facilitate the reproducible targeting of pure spheres, worms and vesicles for this PISA formulation. It is also demonstrated that PDMS-based diblock copolymer worms can be prepared in

hexamethyldisiloxane (HMDS), octamethylcyclotetrasiloxane (D4), and also *n*-dodecane. A potential application for such worm gels as a bespoke thickener for silicone oils is briefly explored.

Experimental

Materials

Monocarbinol terminated $PDMS_{66}$ (M_n = 5,000 g mol^{-1}, mean degree of polymerization = 66) was purchased from Fluorochem (UK) and used as received. D5 and D4 were donated by Scott Bader Company Ltd. (UK). Trigonox 21s (T21s) was purchased from AkzoNobel (The Netherlands). 2-(Dimethylamino)ethyl methacrylate (DMA), HMDS, *n*-dodecane, dichloromethane (DCM), triethyl amine (TEA), butylated hydroxytoluene (BHT), N,N'dicyclohexylcarbodiimide (DCC), 4-dimethylaminopyridine (DMAP), BzMA, 2,2,2-trifluoroethyl methacrylate (TFEMA), methacrylic acid (MAA), 2-phenylethanethiol, sodium hydride (60 % in mineral oil), diethyl ether, carbon disulfide, iodine, sodium thiosulfate, sodium sulfate, ethyl acetate, *n*-hexane, 4,4'-azobis(4-cyanovaleric acid) (ACVA), methyl methacrylate (MMA), tetrahydrofuran (THF) and 2-methoxyethyl methacrylate (MOEMA) were purchased from Sigma Aldrich (UK). Glycerol monomethacrylate (GMA) was kindly donated by GEO Specialty Chemicals (UK) and 2-hydroxypropyl methacrylate (HPMA) was purchased from Alfa Aesar (UK). Chloroform-d, dichloromethane-d_2, and pyridine-d_5 were obtained from Goss Scientific (UK). 4-Cyano-4-(2-phenylethane sulfanylthiocarbonyl) sulfanylpentanoic acid (PETTC) RAFT agent was prepared in-house according to a previously reported protocol.[27,46] DMA was passed through basic alumina prior to use to remove its inhibitor. All other reagents were used as received unless otherwise stated.

Synthesis of the $PDMS_{66}$-TTC macro-CTA

A flame-dried 100 ml round-bottomed flask, equipped with a magnetic follower was charged with 32.0 g (6.4 mmol) of monocarbinol terminated $PDMS_{66}$. The PDMS was stirred for one hour under high vacuum in order to remove any traces of volatile compounds. PETTC (3.68 g, 10.88 mmol), DMAP (88.6 mg,

0.72 mmol), and anhydrous DCM (80 ml) were then added, and the resulting mixture was cooled to 0 °C (ice bath), before being purged with nitrogen gas for 30 min. Whilst keeping the reaction mixture under a positive pressure of nitrogen gas, a cold DCC solution in dry DCM (4.48 g, 21.76 mmol, in 20 ml DCM) was added dropwise over 20 min. After a further hour at 0 °C, the mixture was allowed to warm to room temperature gradually before being heated at 35 °C for 20 h. The reaction was then quenched via exposure to air, filtered to remove the dicyclohexylurea precipitate, and purified via column chromatography (*n*-hexane/DCM, 70/30 v/v as eluent). The yellow product was then dried under vacuum, dissolved in *n*-hexane (100 ml) and washed with methanol (3 x 200 ml) in order to remove any remaining traces of PETTC. The *n*-hexane was removed from the final product under reduced pressure. ^{1}H NMR in CD_2Cl_2 indicated an end-group functionality of 92 % whereas UV Vis indicated a mean functionality of 93 %.

Synthesis of PDMS$_{66}$-PDMA$_x$ diblock copolymer nanoparticles in D5 silicone oil

A representative RAFT dispersion polymerization of DMA in D5 silicone oil targeting a final poly(2-(dimethylamino)ethyl methacrylate) (PDMA) DP of 200 and a final copolymer concentration of 25 % w/w was conducted as follows: A 10 ml glass vial was charged with PDMS$_{66}$-TTC macro-CTA (0.10 g, 18.78 µmol), D5 silicone (2.07 g), DMA monomer (0.59 g, 3.76 mmol) and a magnetic follower. T21s initiator was then added (1.35 mg, 6.26 µmol; added as 10 % v/v stock solution in D5) and the vial was equipped with a rubber septum. The resulting reaction mixture was purged with nitrogen for 20 min, sealed, and then placed in a pre-heated oil bath set at 90 °C for 8 h. ^{1}H NMR analysis in $CDCl_3$ indicated a DMA conversion of 93 %, determined by fixing the signals due to the oxymethylene protons of the PDMA polymer and unreacted DMA monomer (between 3.9 ppm and 4.3 ppm) at 2, and then comparing the intensity of the two signals due to the remaining vinyl protons of the unreacted DMA monomer (at 5.6 and 6.1 ppm). Gel permeation chromatography (GPC) analysis in THF indicated a final M$_n$ of 38,300 g mol^{-1} and a M$_w$/M$_n$ of 1.23, relative to a series of near-monodisperse PMMA calibrants.

Synthesis of PDMS$_{66}$-PDMA$_x$ diblock copolymer worms in D4 silicone oil

PDMS$_{66}$-macro-CTA (0.60 g, 0.11 mmol) was weighed out into a 20 ml reaction vial. D4 silicone oil was added (5.76 g, corresponding to a final copolymer concentration of 30 % w/w), along with DMA monomer (1.86 g, 11.8 mmol) to afford a target PDMA DP of 105. T21s initiator (8.13 mg, 37.6 μmol; added as 10 % v/v stock solution in D4) was then added, and the vial was equipped with a magnetic follower and rubber septum. The reaction mixture was purged with nitrogen gas for 20 min, before being sealed and placed in a pre-heated oil bath set at 90 °C for 6 h. ^{1}H NMR analysis in CDCl$_3$ indicated a DMA conversion of 97 % and THF GPC analysis indicated that M_n = 24,300 g mol^{-1} and M_w/M_n = 1.38.

Synthesis of PDMS$_{66}$-PDMA$_x$ diblock copolymer worms in hexamethyldisiloxane

PDMS$_{66}$-macro-CTA (0.60 g, 0.11 mmol) was weighed out into a 20 ml reaction vial. HMDS was added (6.38 g, corresponding to a final copolymer concentration of 30 % w/w), along with DMA monomer (2.12 g, 13.5 mmol) to afford a target PDMA DP of 120. T21s initiator (8.13 mg, 37.6 μmol; added as 10 % v/v stock solution in hexamethyldisiloxane) was then added, and the vial was equipped with a magnetic follower and rubber septum. The reaction mixture was purged with nitrogen gas for 20 min, before being sealed and placed in a pre-heated oil bath set at 90 °C for 6 h. ^{1}H NMR analysis in CDCl$_3$ indicated a DMA conversion of 92 % and THF GPC analysis indicated that M_n = 26,800 g mol^{-1} and M_w/M_n = 1.34.

Synthesis of PDMS$_{66}$-PDMA$_x$ diblock copolymer worms in *n*-dodecane

PDMS$_{66}$-macro-CTA (0.60 g, 0.11 mmol) was weighed out into a 20 ml reaction vial. *n*-Dodecane was added (5.55 g, corresponding to a final copolymer concentration of 30 % w/w), along with DMA monomer (1.77 g, 11.3 mmol) to afford a target PDMA DP of 100. T21s initiator (8.13 mg, 37.6 μmol; added as 10 % v/v stock solution in *n*-dodecane) was then added, and the vial was equipped with a magnetic follower and rubber septum. The reaction mixture was purged with nitrogen gas for 20 min, before being sealed

and placed in a pre-heated oil bath set at 90 °C for 6 h. ^{1}H NMR analysis in CDCl$_3$ indicated a DMA conversion of 91 % and THF GPC analysis indicated that M_n = 24,600 g mol^{-1} and M_w/M_n = 1.40.

Synthesis of PDMS$_{66}$-stabilized methacrylic diblock copolymer nanoparticles in D5 silicone oil

A typical RAFT polymerization (conducted under either dispersion or emulsion conditions, depending on the particular monomer solubility) was conducted as follows. A 10 ml glass vial was charged with the PDMS$_{66}$-TTC precursor (0.10 g, 18.78 µmol), an appropriate mass of the methacrylic monomer to afford a target DP of 200 [e.g. BzMA (0.33 g, 0.19 mmol)], an appropriate mass of D5 silicone oil for a final copolymer concentration of 25 % w/w solids and T21s initiator (1.30 mg, 6.30 µmol; added as 15 µl of a 10 % v/v stock solution in D5 silicone oil, [macro-CTA]/[T21s] = 3.0). The resulting reaction solution (or emulsion, depending on the monomer solubility in D5) was then purged with nitrogen for 20 min, sealed and placed in a pre-heated oil bath set at 90 °C for 16 h. ^{1}H NMR analysis conducted in CDCl$_3$ (or d5 pyridine in the case of PDMS$_{66}$-PGMA$_{198}$) indicated monomer conversions ranging from 85 % to 98 %. Where possible, THF GPC analysis was conducted, which indicated M_n values ranging from 26,100 g mol-1 to 65,000 g mol-1 and Mw/Mn values between 1.10 and 1.78.

Exhaustive methylation of PDMS$_{66}$-PMAA$_{196}$ diblock copolymers for THF GPC analysis

Prior to analysis by THF GPC, the PDMS$_{66}$-PMAA$_{196}$ diblock copolymers were subject to exhaustive methylation, according to a previously reported protocol.[47] Briefly, excess trimethylsilyldiazomethane was added dropwise to a solution of copolymer (30 mg) in THF (2.0 ml), until a yellow color persisted. The solution was then stirred overnight whilst open to air, such that all of the THF evaporated. The resulting methylated diblock copolymer was then dissolved in THF prior to GPC analysis.

Characterization

^{1}H NMR spectroscopy. ^{1}H NMR spectra were recorded in either d$_5$-pyridine, CDCl$_3$ or CD$_2$Cl$_2$ using a Bruker AV1-400 MHz spectrometer. Typically, 64 scans were averaged per spectrum.

GPC. Molecular weight distributions were determined using a GPC instrument operating at 30 °C that comprised two Polymer Laboratories PL gel 5 μm Mixed C columns, a LC20AD ramped isocratic pump, THF eluent and a WellChrom K-2301 refractive index detector operating at 950 ± 30 nm and a variable wavelength UV-visible detector operating at 298 nm. The mobile phase contained 2.0 % v/v TEA and 0.05 % w/v BHT; the flow rate was fixed at 1.0 mL min^{-1} and toluene was used as a flow rate marker. A series of ten near-monodisperse poly(methyl methacrylate) (PMMA) standards (M_n = 1 280 to 330 000 g mol^{-1}) were used for calibration. Chromatograms were analyzed using Varian Cirrus GPC software.

Dynamic light scattering. Dynamic light scattering (DLS) studies were performed using a Zetasizer Nano-ZS instrument (Malvern Instruments, UK) at 25 °C at a fixed scattering angle of 173°. Copolymer dispersions were diluted in the solvent in which they were synthesized (typically D5) to a final concentration of 0.10 % w/w. The z-average diameter and polydispersity (PDI) of the diblock copolymer particles were calculated by cumulants analysis of the experimental correlation function using Dispersion Technology Software version 6.20. Data were averaged over ten runs each of thirty seconds duration.

Transmission electron microscopy. Transmission electron microscopy (TEM) studies were conducted using a FEI Tecnai G2 spirit instrument operating at 80 kV and equipped with a Gatan 1k CCD camera. Copper TEM grids were surface-coated in-house to yield a thin film of amorphous carbon. The grids were then loaded with 0.05-0.25 % w/w copolymer dispersions precooled to 3 °C and then allowed to dry at this temperature within a refridgerator overnight. Given the relatively low T_g of the PDMA block, such conditions were found to be necessary in order to preserve the original copolymer morphology. Prior to imaging, each grid was exposed to ruthenium (IV) vapor for 7 min at ambient temperature, in order to improve contrast. The ruthenium oxide stain was prepared by adding ruthenium (II) oxide (0.3 g) to water (50 g), to form a slurry. Then, sodium periodate (2.0 g) was added whilst stirring to form a yellow solution of ruthenium (IV) oxide within 1 minute.[48] In every case, copolymer dispersions were diluted using the

solvent in which they were synthesized, e.g. $PDMS_{66}$-$PDMA_{100}$ worms prepared in D5 were diluted using D5 etc.

Rheology studies. An AR-G2 rheometer equipped with a 40 mm 2° aluminum cone was used for all measurements. The storage and loss moduli were determined either as a function of strain at a fixed angular frequency of 1.0 rad s^{-1} or as a function of angular frequency at a fixed strain of 1.0 %. In all cases, the gap between the cone and plate was 58 μm. For viscosity measurements, rotational rheometry was used at a fixed shear rate of 10 s^{-1}.

UV-visible Spectroscopy. UV−visible absorption spectra were recorded between 200 and 800 nm using a PC-controlled UV-1800 spectrophotometer at 25 °C using a 1 cm path length quartz cell. A Beer−Lambert calibration curve was constructed using a series of twelve PETTC solutions in dichloromethane. The absorption maximum at 298 nm assigned to the trithiocarbonate group was used for this calibration plot, with PETTC concentrations ranging from 1.2 x 10^{-5} mol dm^{-3} to 1.0 x 10^{-4} mol dm^{-3}. The mean DP for the $PDMS_{66}$-TTC macro-CTA was determined using the molar extinction coefficient of 10153 ± 220 mol^{-1} dm^3 cm^{-1} determined for the PETTC RAFT agent.

Small-angle X-ray scattering (SAXS)

Spheres and Worms. SAXS patterns were recorded at a synchrotron source (ESRF, station ID02, Grenoble, France) using monochromatic X-ray radiation (wavelength $\lambda = 0.0995$ nm, with q ranging from 0.004 to 2.5 nm^{-1}, where $q = 4\pi \sin \theta/\lambda$ is the length of the scattering vector and θ is one-half of the scattering angle) and a Rayonix MX-170HS Kodak CCD detector. Measurements were conducted on 1.0% w/w dispersions. X-ray scattering data were reduced and normalized using standard routines by the beamline.

Vesicles. SAXS patterns were recorded at a synchrotron source (Diamond Light Source, station I22, Didcot, UK) using monochromatic X-ray radiation (wavelength $\lambda = 0.124$ nm, with q ranging from 0.015 to 1.3 nm^{-1}, where $q = 4\pi \sin \theta / \lambda$ is the length of the scattering vector and θ is one-half of the scattering angle) and a 2D Pilatus 2M pixel detector (Dectris, Switzerland). Measurements were conducted on 1.0% w/w dispersions. X-ray scattering data were reduced and normalized using standard routines by the beamline.

Results and Discussion

The monocarbinol PDMS$_{66}$-OH precursor was esterified using a carboxylic acid-functionalized trithiocarbonate RAFT agent (PETTC) via DCC/DMAP coupling in dichloromethane according to a previously reported protocol.[21] The macro-CTA was purified via column chromatography, and GPC with a UV detector operating at 298 nm confirmed the complete removal of any unreacted PETTC (see **Figure S1**). ^{1}H NMR and UV-visible spectroscopy were each used to characterize the resulting PDMS$_{66}$-TTC macro-CTA. In the former case, the five aromatic protons assigned to the RAFT end-group were compared to the integrated PDMS$_{66}$ backbone signal, indicating a mean degree of esterification of 92 ± 5 % (see **Figure 1**). In the latter case, a linear Beer-Lambert calibration curve recorded at a maximum wavelength of 298 nm indicated a mean degree of esterification of 93 ± 5 % (see **Figure S2**).
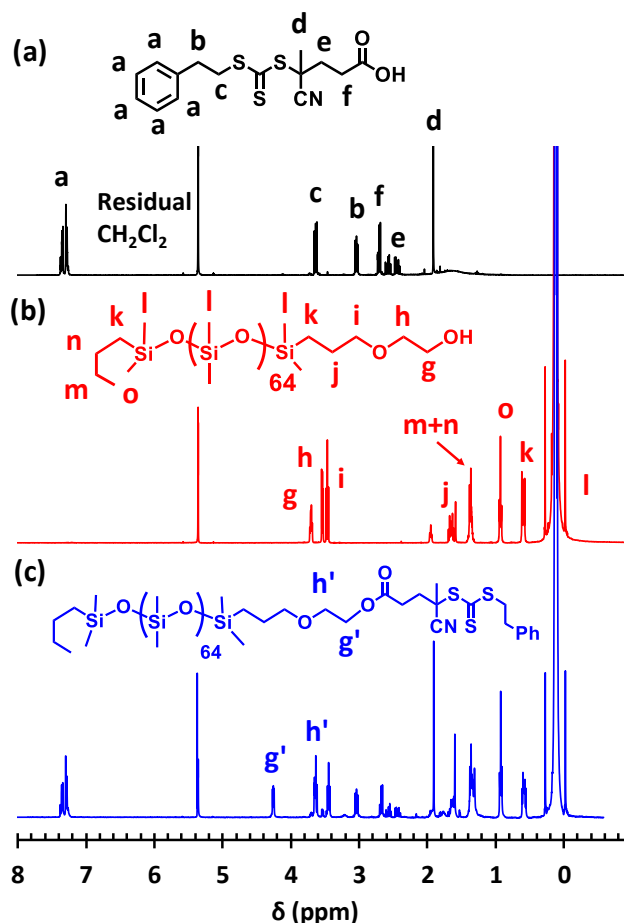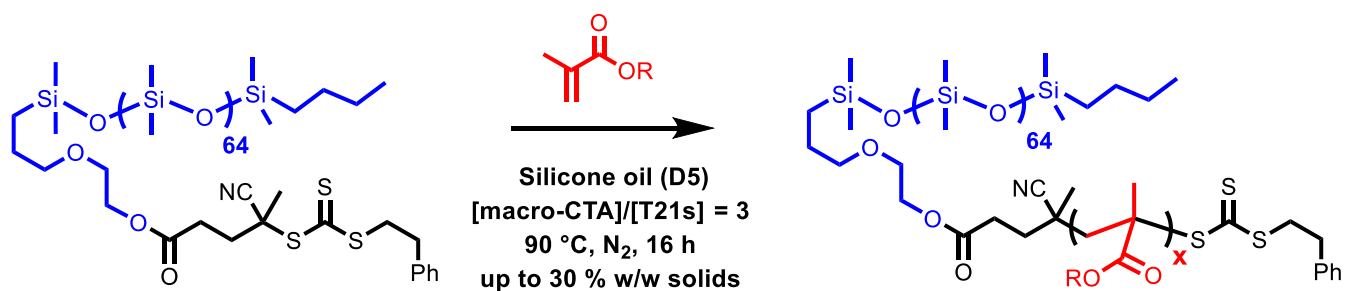
Figure 1. ^{1}H NMR spectra recorded in CD_2Cl_2 for: (a) the PETTC chain-transfer agent (CTA), (b) the monocarbinol-terminated $PDMS_{66}$-OH precursor, and (c) the final $PDMS_{66}$-TTC macro-CTA.

The $PDMS_{66}$-TTC precursor was chain-extended in D5 silicone oil (see **Scheme 1**) using eight different methacrylic monomers in turn, with target diblock copolymer compositions being summarized in **Table 1**.

Scheme 1. RAFT dispersion polymerization of a generic methacrylic monomer in D5 at 90 °C using the $PDMS_{66}$-TTC macro-CTA.

13

Table 1. Summary of the eight methacrylic monomers examined as structure-directing blocks for RAFT dispersion polymerization syntheses conducted in D5 silicone oil at 90 °C using a $PDMS_{66}$-TTC precursor block. In all cases, the copolymer concentration was fixed at 25 % w/w solids and the [macro-CTA]/[T21s] molar ratio = 3.0. An 'X' in the M_n and M_w/M_n columns denotes that GPC analysis was not performed because no common GPC solvent could be identified for the specific diblock copolymer.

Core-forming monomer	Target DP	Conditions	Conv. (%)[a]	M_n / g mol^{-1}	M_w/M_n	Z-avg. diameter /nm (PDI)	TEM morphology
2-(Dimethylamino)ethyl methacrylate	200	Dispersion	93	38,300	1.23	363 (0.3)	Vesicles
Benzyl methacrylate	200	Dispersion	98	36,300	1.22	51 (0.02)	Spheres
2,2,2,-Trifluoroethyl methacrylate	200	Dispersion	98	32,000	1.47	65 (0.25)	Spheres
Methyl methacrylate	200	Dispersion	85	26,100	1.10	32 (0.4)	Spheres
2-Methoxyethyl methacrylate	200	Dispersion	99	34,000	1.34	42 (0.05)	Spheres
Methacrylic acid	200	Dispersion	98	42,200	1.78[c]	277 (0.25)	Ill-defined
2-Hydroxypropyl methacrylate	200	Dispersion[b]	91	65000	1.50	202 (0.4)	Spheres
Glycerol monomethacrylate	200	Emulsion	98	X	X	99 (0.02)	Spheres

[a] ^{1}H NMR spectra were recorded in either $CDCl_3$ or d_5-pyridine. [b] HPMA monomer was immiscible with D5 at room temperature but miscible at reaction temperature. [c] THF GPC analysis was performed after exhaustive methylation with trimethylsilyldiazomethane

For each PISA synthesis, the target DP for the structure-directing methacrylic block and the copolymer concentration were fixed at 200 and 25 % w/w solids, respectively. These conditions were selected because it was previously reported that $PDMS_{66}$-$PBzMA_{200}$ diblock copolymers prepared at 25 % w/w in another non-polar solvent (*n*-heptane) occupy vesicle phase space. Thus, in principle this target DP should be sufficient to also produce vesicular morphologies in D5 silicone oil. In each case, the final copolymer morphology was determined via post mortem TEM studies (**Figure 2**).
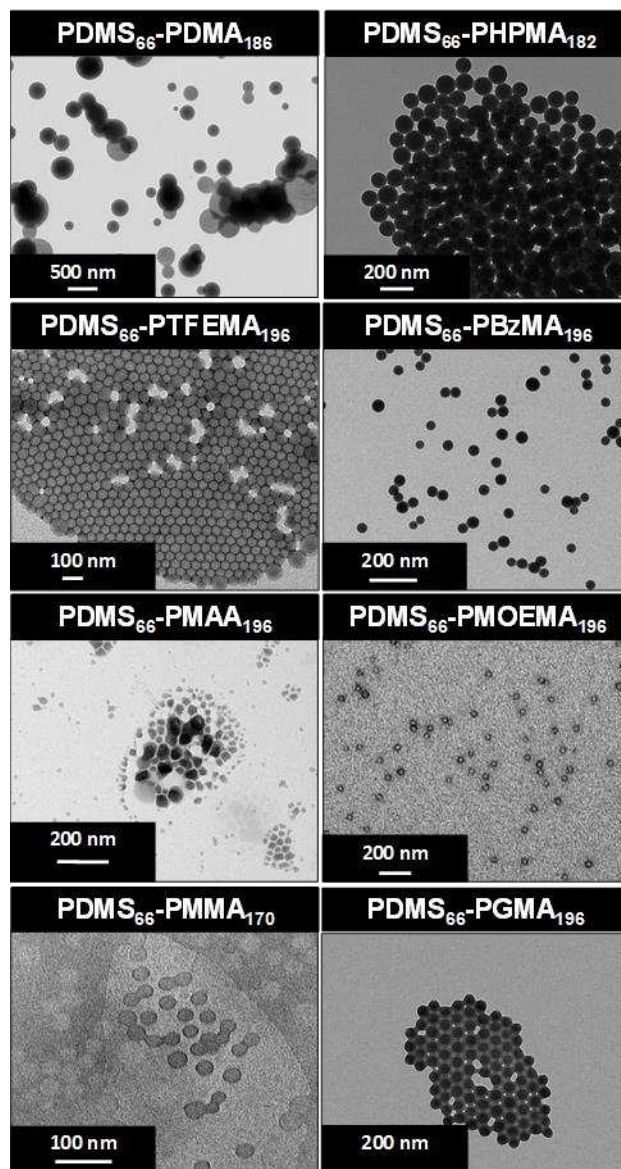
Figure 2. TEM images obtained for the PISA synthesis of diblock copolymer nanoparticles prepared in D5 silicone oil via chain extension of a $PDMS_{66}$ macro-CTA using various methacrylic monomers at 25 % w/w copolymer concentration. PDMA = poly(2-(dimethylamino)ethyl methacrylate), PHPMA = poly(2-hydroxypropyl methacrylate), PMMA = poly(methyl methacrylate), PTFEMA = poly(2,2,2,-trifluoroethyl methacrylate), PBzMA = poly(benzyl methacrylate), PMAA = poly(methacrylic acid), PGMA = poly(glycerol monomethacrylate) and PMOEMA = poly(2-methoxyethyl methacrylate).

Inspection of **Figure 2** and **Table 1** reveals that the only methacrylic monomer that enables access to copolymer morphologies other than spheres (or ill-defined aggregates) in these initial scouting

15

experiments is DMA. A likely explanation for this observation is that PDMA has a glass transition temperature (T_g) of approximately 18 °C,[49] which is significantly lower than the other methacrylic polymers shown in Table 2. This means that the growing PDMA chains have greater mobility within the nanoparticle cores, which is expected to facilitate the evolution in copolymer morphology that is required to avoid kinetically-trapped spheres.[13] Nevertheless, it is perhaps surprising that the PISA synthesis of $PDMS_{66}$-$PBzMA_{200}$ nanoparticles in D5 is restricted to spheres.[21] This is because the full range of copolymer morphologies (spheres, worms or vesicles) can be obtained when conducting the same PISA synthesis in *n*-heptane. Kinetically-trapped spheres are well-documented for RAFT aqueous emulsion polymerization syntheses,[24,26,50,51] but are much less common for RAFT dispersion polymerization formulations unless the mean degree of polymerization of the stabilizer block is sufficiently high to prevent efficient sphere-sphere fusion.[52] However, in the present case it has already been established that the $PDMS_{66}$-TTC precursor is *not* too long to prevent the formation of either worms or vesicles for RAFT dispersion polymerization syntheses conducted in *n*-heptane.[21] Presumably, the kinetically-trapped spheres observed in the present study simply reflect the poorer solvating power of the D5 solvent for the growing PBzMA chains relative to that of *n*-heptane.

A kinetic study was then performed targeting a diblock copolymer composition of $PDMS_{66}$-$PDMA_{200}$ vesicles at 25 % w/w solids using a $PDMS_{66}$-TTC/initiator molar ratio of 3.0. This was achieved by removing small aliquots from the polymerizing reaction mixture at regular time intervals. ^{1}H NMR studies of the declining vinyl monomer signals (relative to the methacrylic backbone signals) revealed that 87 % DMA conversion was attained within 4 h at 90 °C (see **Figure 3a**).
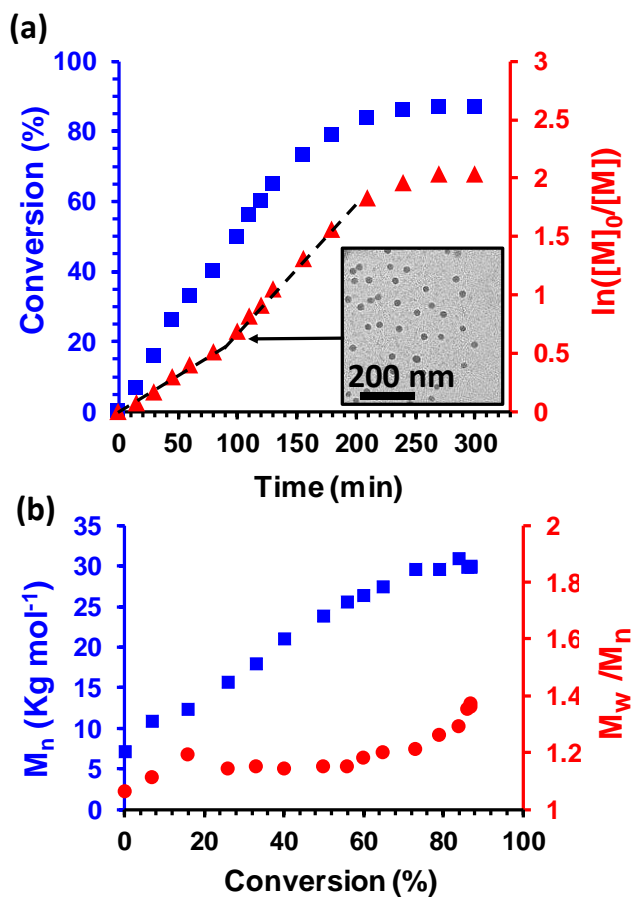
Figure 3. (a) Conversion vs. time curve (blue squares) and the corresponding semi-logarithmic plot (red triangles) for the RAFT dispersion polymerization of DMA at 90 °C using a $PDMS_{66}$ macro-CTA at 25 % w/w solids when targeting a PDMA block DP of 200. The inset TEM image was obtained from an aliquot of the reaction mixture removed after 100 min. (b) Evolution of M_n (blue squares) and M_w/M_n (red circles) with DMA conversion as determined by gel permeation chromatography (THF eluent; calibration against a series of near-monodisperse PMMA standards).

According to the semi-logarithmic plot displayed in **Figure 3a**, an approximate two-fold increase in the rate of DMA polymerization was observed at around 80-100 min, which corresponds to a DMA conversion of 40 to 50 % (and hence an intermediate diblock copolymer composition of $PDMS_{66}$-$PDMA_{80-100}$). In the PISA literature, such a rate enhancement normally corresponds to the onset of micellar nucleation.[53–55] In contrast, in the present case the rate acceleration *appeared* to occur after the nucleation event. This interpretation was based on the observation that an aliquot extracted at 100 min

17

formed a physical gel at 20 °C, indicating the presence of weakly interacting worms (which are believed to be formed via multiple 1D fusion of the initial spherical micelles).[55] However, as pointed out by two reviewers of this manuscript, if the growing PDMA blocks are sufficiently solvated at 90 °C then the rate acceleration observed after approximately 80-100 min may actually correspond to the formation of nascent spherical micelles (rather than worms). To examine this hypothesis, we repeated the kinetics experiment and an aliquot was extracted at 100 min, i.e. just after the onset of micellar nucleation (see Figure 3). This aliquot was diluted approximately one hundred-fold at 90 °C using hot D5 solvent, cooled to 3 °C and then a TEM grid was prepared using the resulting dilute dispersion. This protocol is expected to quench the DMA polymerization and kinetically trap the evolving copolymer morphology. It produced the image shown as an inset within Figure 3, which confirms that the predominant copolymer morphology just after the rate acceleration event is actually spheres. Thus this PISA formulation is no different to many other systems discussed in the literature.[55–57] Thus it seems likely that the few cases where the onset of micellization has apparently coincided with the presence of higher order morphologies (rather than the formation of spheres) are actually artifacts caused by the ingress of hot solvent at elevated temperature into the nanoparticle cores.[21,58–60]

Each aliquot removed for these kinetic studies was also analyzed via GPC to assess the evolution of M_n and M_w/M_n during the DMA polymerization (see **Figure 3b**). A linear evolution of M_n with conversion was observed, as expected for a RAFT polymerization. However, the dispersity (M_w/M_n) gradually increased with conversion, although it remained below 1.40 throughout the polymerization. Moreover, the blocking efficiency is relatively high and each GPC trace is unimodal (see **Figure S3**).

Several further series of PDMS$_{66}$-PDMA$_x$ diblock copolymers were prepared by systematically varying the target PDMA DP and the copolymer concentration. In each case the final copolymer morphology was assessed by TEM in order to construct a phase diagram (see **Figure 4).** Below a PDMA DP of 20, no nanoparticles were obtained because the PDMA blocks were too short to induce micellar nucleation. At

relatively low copolymer concentrations (e.g. 10 or 15 %), spherical micelles were obtained when targeting PDMA DPs below 100 and vesicles were produced for PDMA DPs greater than 170. At intermediate PDMA DPs (e.g. 100 – 170) mixed phases resulted, i.e. no pure worm phase could be isolated at these copolymer concentrations. In contrast, the full range of copolymer morphologies (spheres, worms or vesicles) could be obtained when PISA syntheses were conducted at 25 % w/w solids or above.
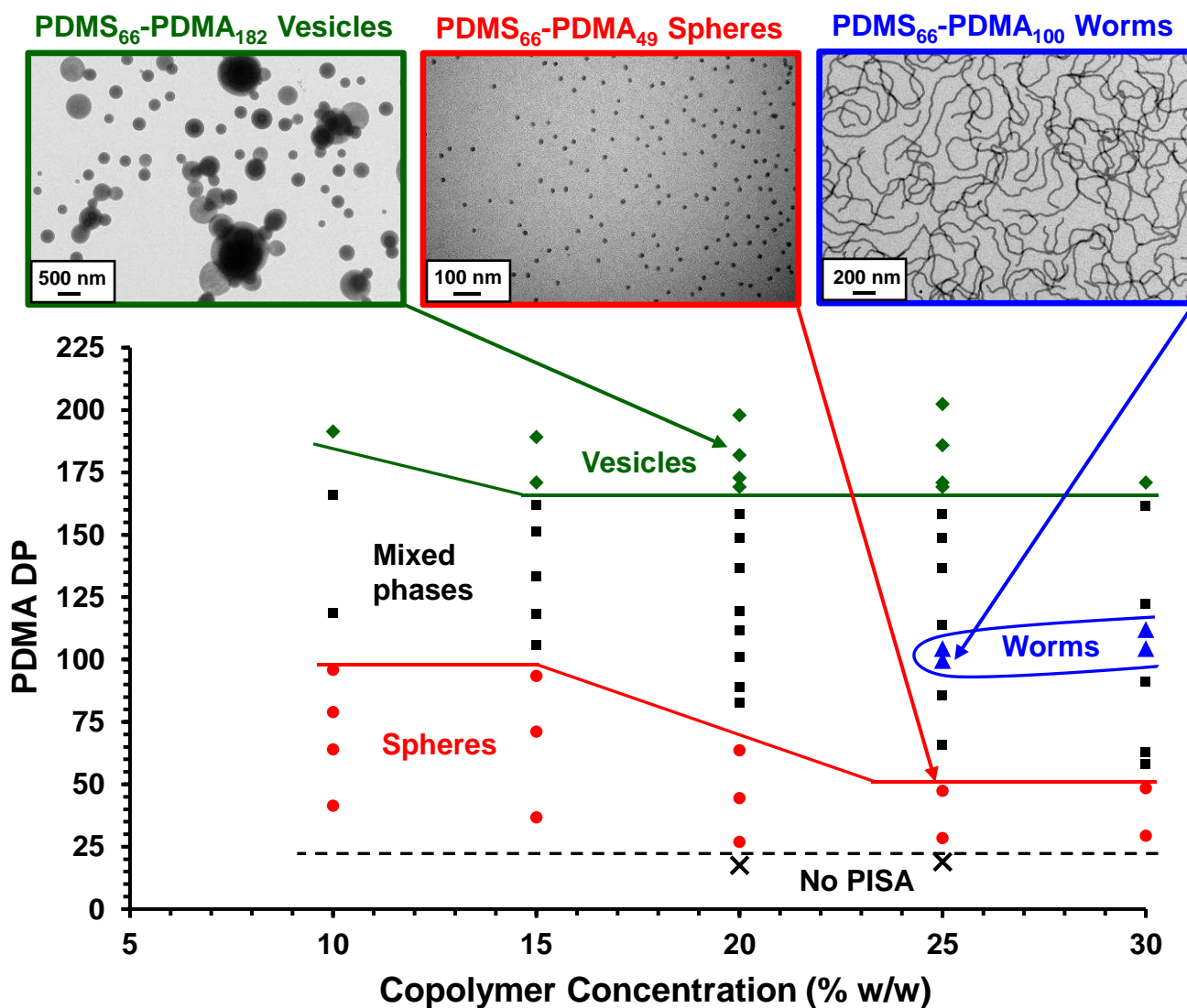

Figure 4. Phase diagram constructed for $PDMS_{66}$-$PDMA_x$ diblock copolymer nanoparticles prepared by RAFT dispersion polymerization of DMA in D5 using a $PDMS_{66}$-TTC RAFT agent and T21s as an initiator ([$PDMS_{66}$-TTC]/[T21s] molar ratio = 3.0). A representative TEM image for each pure copolymer morphology is also shown.

Spheres had mean core diameters ranging from 23 nm to 46 nm as determined by DLS, depending on the DP of the core-forming block and the copolymer concentration at which the synthesis was conducted. Well-defined worms with a mean cross-sectional diameter of around 26 nm ± 2 nm were obtained for PDMA DPs ranging between 100 and 112, while polydisperse vesicles were obtained for PDMA DPs of 169 or higher.

The T_g of PDMA lies just below ambient temperature,[49] so it was difficult to obtain high resolution TEM images of the diblock copolymer nano-objects, even when preparing the TEM grids at 3 °C. This is particularly evident for the putative vesicles shown in **Figure 4**, where it proved rather difficult to verify the presence of vesicle membranes. To address this technical problem, three examples of apparently pure $PDMS_{66}$-$PDMA_x$ spheres, worms and vesicles (as judged by TEM) were subjected to further characterization by SAXS using international synchrotron facilities (see Figure 5). Compared to TEM, the latter technique provides much more robust structural information, because X-ray scattering is averaged over many millions of nanoparticles. Furthermore, SAXS analysis can be conducted directly on dispersions, so problems associated with the low T_g of the PDMA block are avoided.

It is well-known[21,61] that the dominant copolymer morphology can be inferred by inspecting the gradient of an $I(q)$ vs. q plot in the low q region, where q is the scattering vector ($q = 4\pi\sin\theta/\lambda$) and $I(q)$ is the X-ray scattering intensity. The scattering pattern obtained for $PDMS_{66}$-$PDMA_{49}$ nanoparticles exhibits a gradient of approximately zero (**Figure 5a**), which is consistent with the well-defined spherical morphology indicated by TEM in this case. Accordingly, fitting this scattering pattern to a well-known spherical micelle model enables calculation of the volume-average sphere core diameter, which was determined to be 16.5 nm. Given that the radius of gyration of the PDMS steric stabilizer block is approximately 1.7 nm, this corresponds to an overall volume-average diameter of 23 nm, which is slightly lower than the intensity-average DLS diameter of 28 nm but greater than the TEM number-average

diameter of 19 nm (estimated by analyzing 100 nanoparticles). Furthermore, the mean aggregation number of these $PDMS_{66}$-$PDMA_{49}$ spheres was estimated to be 196.
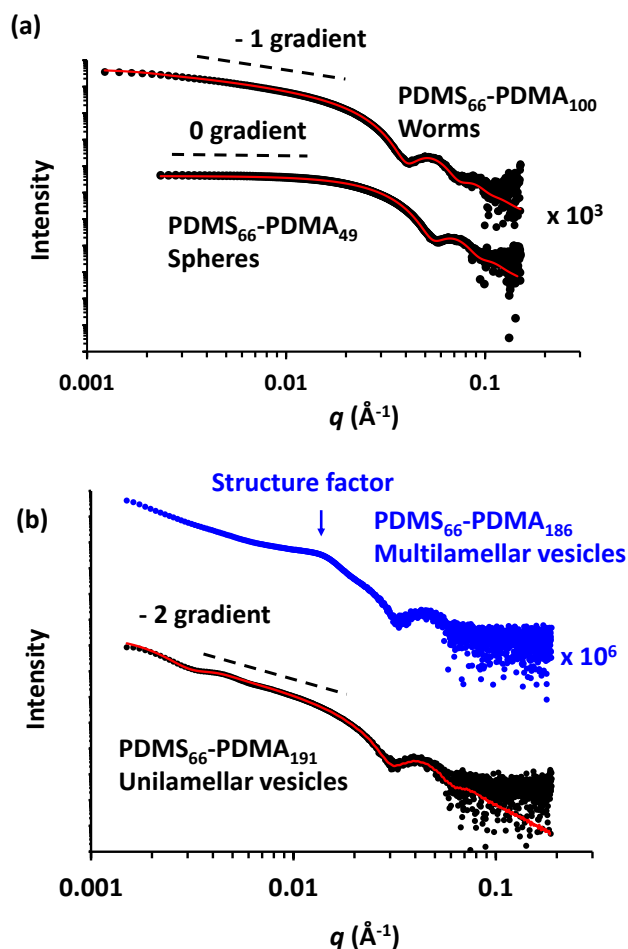

Figure 5. (a) SAXS patterns (black data; recorded at 1.0 % w/w solids in D5 silicone oil) obtained for $PDMS_{66}$-$PDMA_{49}$ spheres and $PDMS_{66}$-$PDMA_{100}$ worms, both originally synthesized at 25 % w/w solids in D5 via RAFT dispersion polymerization of DMA at 90 °C. Data fits are shown as red lines and were obtained using an appropriate sphere or worm model. (b) SAXS patterns (recorded at 1.0 % w/w solids in D5 silicone oil) for $PDMS_{66}$-$PDMA_{191}$ unilamellar vesicles (black data) originally synthesized at 10 % w/w in D5, and $PDMS_{66}$-$PDMA_{186}$ multilamellar vesicles (blue data) originally synthesized at 25 % w/w in D5. The data fit to the $PDMS_{66}$-$PDMA_{191}$ unilamellar vesicle pattern was obtained using an appropriate vesicle model (see red line). No satisfactory fit could be obtained for the pattern recorded for the multilamellar vesicles owing to the presence of a structure factor at intermediate q (see blue arrow).

The low q gradient of the scattering pattern recorded for PDMS$_{66}$-PDMA$_{100}$ is approximately -1 (**Figure 5a**), which is characteristic of highly anisotropic worm-like particles.[21] This is consistent with TEM studies, which indicate that this diblock composition forms a pure worm phase. Fitting this scattering pattern to an appropriate worm model[62] indicates a mean worm cross-sectional diameter of 25 nm, which correlates reasonably well with the mean worm thickness of 26 ± 2 nm estimated from TEM studies. Unfortunately, the overall worm contour length could not be determined from this scattering pattern, because the accessible q range for the ID02 instrument set-up was not sufficiently low. However, inspection of TEM images suggests a mean worm contour length of at least 1.5 µm (see **Figure S4**). Several PISA syntheses of PDMS$_{66}$-PDMA$_{x}$ diblock copolymer nano-objects were conducted targeting higher x values at several copolymer concentrations. In each case, a vesicular morphology was anticipated. However, as mentioned above, TEM studies indicated the formation of large, polydisperse spherical particles but did not provide convincing evidence for vesicular membranes (see **Figure 4**). Fortunately, SAXS studies enabled confirmation of the expected vesicular morphologies. For example, the black curve in **Figure 5b** corresponds to a PISA synthesis conducted at 10% w/w copolymer concentration when targeting PDMS$_{66}$-PDMA$_{220}$. In this case, the low q gradient was calculated to be approximately -2 and the local minimum suggested a mean vesicle membrane thickness of 21 nm. This particular scattering pattern could be well-fitted using a unilamellar vesicle model, which indicated an overall vesicle diameter of 206 nm and a mean aggregation number of 48,337. Targeting a similar diblock copolymer composition at 25% w/w copolymer concentration led to a distinctive structure factor at intermediate q (blue pattern, **Figure 5b**), which is consistent with the formation of multilamellar vesicles.[25] This structural feature complicates the SAXS analysis, which is beyond the scope of the current work. However, TEM studies provide further evidence for the formation of multilamellar vesicles in this case (see **Figure S5**). The various structural parameters calculated for the SAXS patterns shown in **Figure 5** are summarized in **Table S2**.

To assess the evolution of molecular weight on varying the PDMA DP at 25 % w/w copolymer concentration, selected samples were analyzed by GPC (see **Figure 6**). Each GPC curve was unimodal, indicating a high blocking efficiency. Furthermore, M_w/M_n values remained below 1.25 for target PDMA DPs up to 220, indicating that these additional DMA polymerizations were also reasonably well-controlled. However, the weak high molecular weight shoulder observed in the GPC trace recorded for PDMS$_{66}$-PDMA$_{48}$ (see red trace in Figure 6) becomes increasingly prominent when targeting shorter PDMA blocks (see Figure S6a).
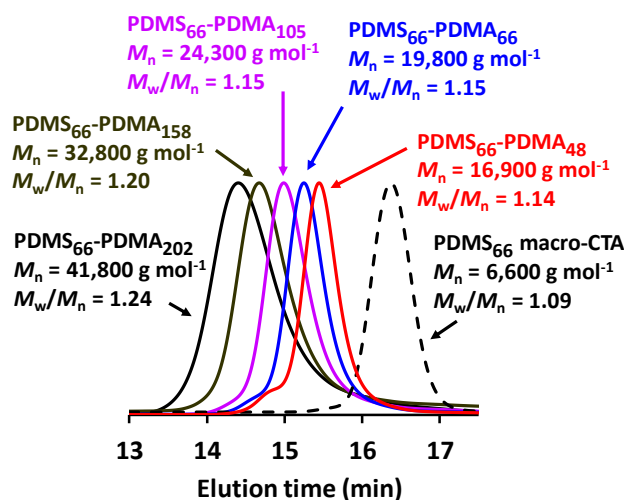

Figure 6. GPC traces obtained using a refractive index detector (THF eluent; calibrated using a series of near-monodisperse PMMA standards) recorded for the PDMS$_{66}$-TTC precursor (black dashed curve) and a series of PDMS$_{66}$-PDMA$_x$ diblock copolymers prepared at 25 % w/w solids in D5 silicone oil while targeting an increasing degree of polymerization for the PDMA block.

Such bimodal distributions proved to be reproducible and UV GPC analysis ($\lambda = 298$ nm) indicated that the RAFT end-group remains attached to these higher molecular weight chains (see Figure S6b). Moreover, this feature has approximately twice the molecular weight compared to the main peak. One plausible explanation is that chain transfer to the PDMA block occurs when using the relatively high initiator concentration required for such PISA syntheses. We emphasize that these observations have essentially no bearing on the main findings of this manuscript.

The PDMS$_{66}$-PDMA$_{100-112}$ diblock copolymer worms prepared at 25 – 30 % w/w solids formed soft, free-standing gels on cooling to ambient temperature. To examine the physical properties of such worm gels, a 30 % w/w PDMS$_{66}$-PDMA$_{105}$ worm dispersion in D5 silicone oil was analyzed via oscillatory rheology. First, the effect of varying the applied strain on the storage (G') and loss (G'') modulus was determined (see **Figure 7a**).
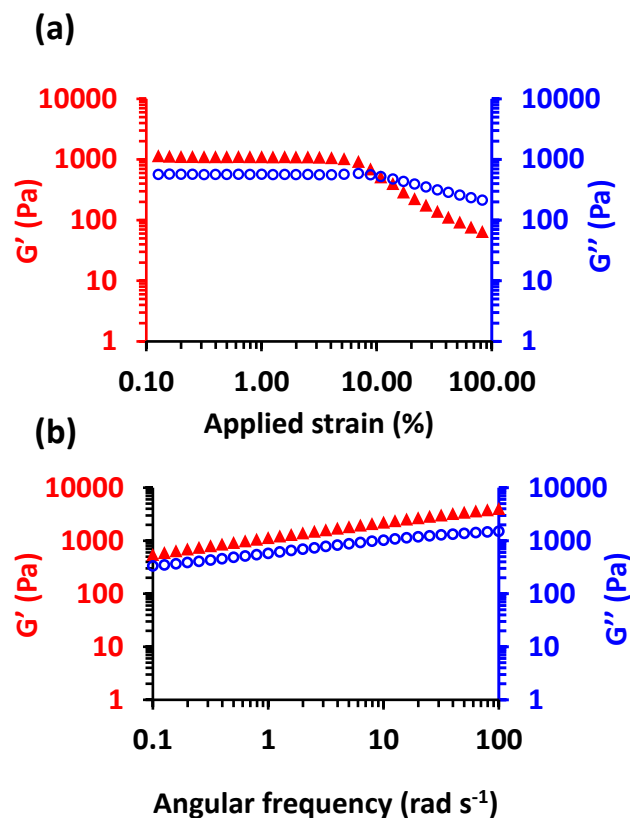

Figure 7. (a) Effect of varying the applied strain on the storage moduli (G'; filled red triangles) and loss moduli (G''; open blue circles). (b) Effect of varying the angular frequency on the storage moduli (G'; filled red triangles) and loss moduli (G''; open blue circles).

The plateau region observed for G' and G'' below 10 % strain confirmed the viscoelastic nature of this worm gel. For strains exceeding 10 %, the magnitude of G' falls below G'', indicating the yield point.[63] For a truly viscoelastic material, G' and G'' should be independent of the applied frequency. Hence, the

effect of varying the applied frequency between 0.1 and 100 rad s^{-1} on the gel properties was also assessed (**Figure 7b**). However, for PDMS$_{66}$-PDMA$_{105}$ worms prepared in D5 silicone oil, a modest increase in both G' and G'' was observed on increasing the applied frequency. This has been observed for certain other worm gels prepared via PISA and suggests some deviation from ideal viscoelastic behavior.[25,64] To assess the critical gelation concentration (CGC) of the PDMS$_{66}$-PDMA$_{105}$ worms, a larger scale batch was prepared at 30 % w/w solids. Aliquots were diluted using D5 silicone oil via gentle stirring overnight to achieve copolymer concentrations ranging from 5 to 25 % w/w solids. The resulting dispersions were then assessed via oscillatory rheology at a fixed strain of 1.0 % and an angular frequency of 1 rad s^{-1} in order to determine G' and G'' in each case (see **Figure 8**).
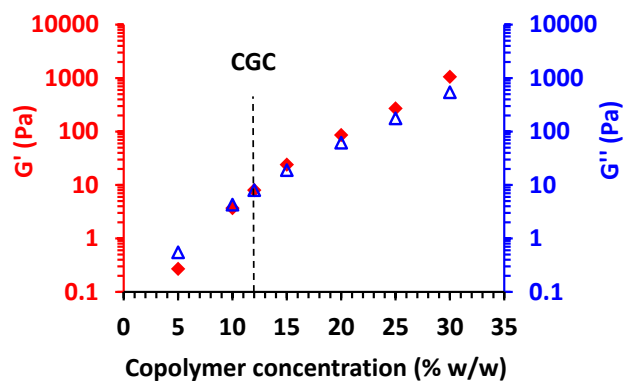

Figure 8. (a) Concentration dependence of the storage moduli (G'; filled red diamonds) and loss moduli (G''; open blue triangles) determined for a series of PDMS$_{66}$-PDMA$_{105}$ worm dispersions. The critical gelation concentration (CGC) is indicated by the dashed black line.

Inspecting **Figure 8**, G' exceeds G'' for copolymer concentrations greater than 12 % w/w, indicating that these worm dispersions are physical gels. On the other hand, G' is less than G'' for copolymer concentrations below 12 % w/w, indicating free-flowing fluids in this case. At 12 % w/w, the magnitude

of G' and G'' are equivalent, hence, the CGC for $PDMS_{66}$-$PDMA_{105}$ worm-gels is estimated to be 12 % w/w copolymer concentration. This is consistent with CGC values reported for related PISA syntheses of diblock copolymer worms in non-polar media.[20]

In addition to D5 silicone oil, $PDMS_{66}$-$PDMA_x$ worm-gels were also synthesized at 30 % w/w solids in three other non-polar solvents, namely D4 silicone oil, HMDS and *n*-dodecane. The critical DP required for the PDMA block to obtain worms in each solvent differed slightly, but not by more than twenty units. A summary of these various PISA formulations is provided in Table 2, along with the storage moduli (G') and critical gelation concentration (CGC) observed for each copolymer-solvent pair. Representative TEM images are shown in **Figure 9.**

Table 2: Summary of the storage modulus (G') and critical gelation concentration (CGC) for four $PDMS_{66}$-$PDMA_x$ worm gels prepared via RAFT dispersion polymerization of DMA at 30 % w/w solids in various solvents.

Solvent	Copolymer Composition	G' at 20 °C (Pa)	CGC (% w/w)
D5	$PDMS_{66}$-$PDMA_{105}$	1057	12
D4	$PDMS_{66}$-$PDMA_{102}$	677	12
n-dodecane	$PDMS_{66}$-$PDMA_{91}$	845	10
HMDS	$PDMS_{66}$-$PDMA_{110}$	450	14

a) n-dodecane $PDMS_{66}-PDMA_{91}$

200 nm

b) HMDS $PDMS_{66}-PDMA_{110}$

500 nm

c) D4 $PDMS_{66}-PDMA_{102}$

500 nm

d) D5 $PDMS_{66}-PDMA_{105}$

1 µm

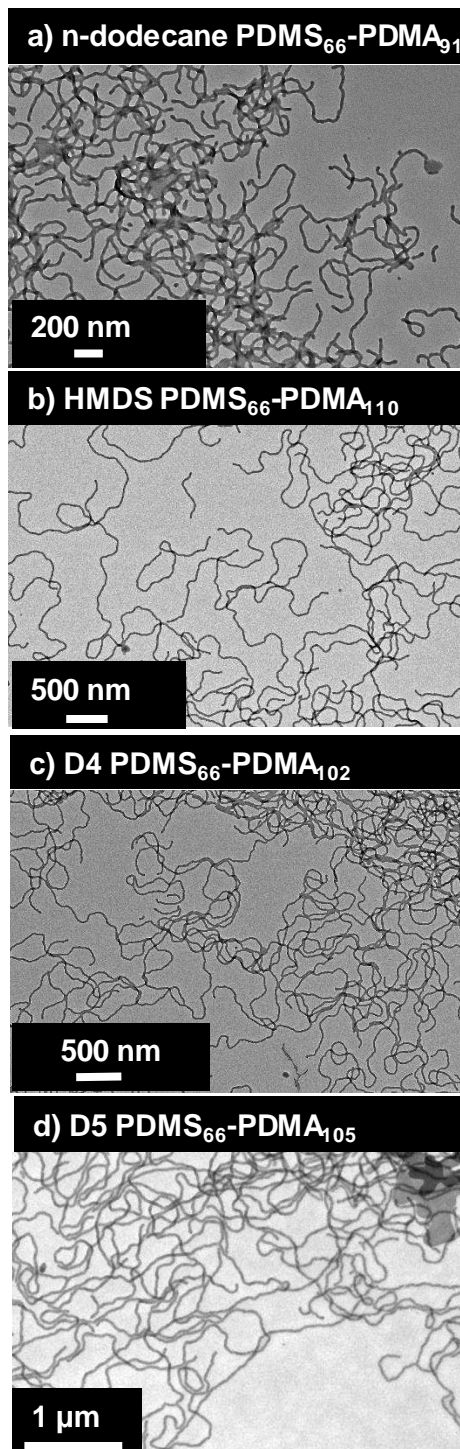**Figure 9**. TEM images obtained for a series of $PDMS_{66}-PDMA_x$ worms prepared at 30 % w/w copolymer concentration in various solvents.

Finally, the viscosity-modifying performance of PDMS$_{66}$-PDMA$_x$ worms was investigated in each of these four solvents over a copolymer concentration range of 5 to 30 % w/w solids. The viscosity for each dispersion was determined via rotational rheometry at a fixed shear rate of 10 s^{-1} (see **Figure 10**). Clearly, only a relatively low concentration ($\sim$ 5 % w/w) of PDMS$_{66}$-PDMA$_x$ worms is required to produce a sixty-fold increase in solution viscosity relative to the corresponding pure solvent. Higher copolymer concentrations lead to a viscosity enhancement by well over four orders of magnitude. Such observations suggest that PDMS$_{66}$-PDMA$_x$ worms may be useful as viscosity modifiers for non-polar oils, especially silicones.
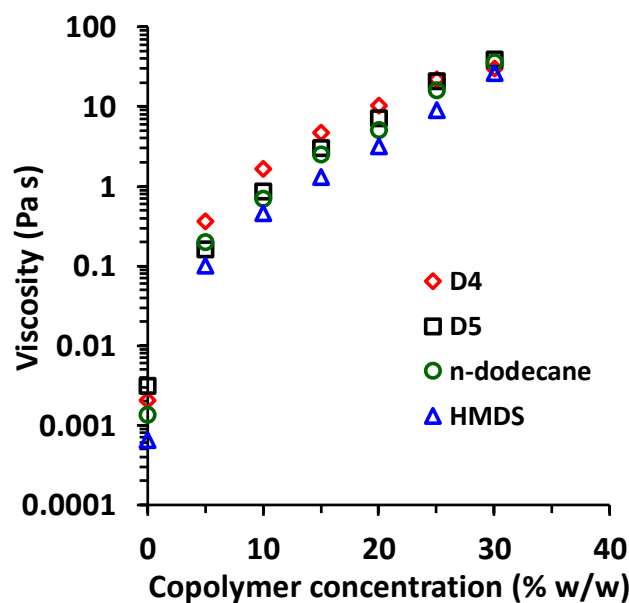

Figure 10. Concentration dependence of the solution viscosity (determined at a fixed shear rate of 10 s^{-1}) determined for PDMS$_{66}$-PDMA$_x$ diblock copolymer worms prepared in either D5 silicone oil (open black squares), D4 (open green diamonds), HMDS (open blue triangles) or *n*-dodecane (open red circles), where x varies between 91 and 110 depending on the solvent type. In each case, worms were prepared at an initial copolymer concentration of 30 % w/w solids and then sequentially diluted using the same solvent for viscosity measurements. The precise PDMA target DP required to produce a pure worm phase varied slightly according to the solvent: the actual diblock compositions in each case are shown in **Table 2.**

Conclusions

A well-defined PDMS$_{66}$-TTC precursor was prepared with a high degree of end-group functionality using a previously reported esterification protocol.[21] Chain extension was examined with a range of methacrylic monomers via PISA formulations conducted in D5 silicone oil. Perhaps surprisingly, only DMA provided access to the full range of copolymer morphologies (spheres, worms or vesicles), with all other methacrylic monomers leading to the formation of kinetically-trapped spheres. A likely explanation for this unexpected difference is the relatively low T_g of the PDMA chains. However, this does not account for the observation of kinetically-trapped spheres in the case of BzMA, for which the full range of copolymer morphologies has been reported for PISA syntheses when using precisely the same PDMS-TTC precursor block in another non-polar solvent (*n*-heptane).[21] It is also noteworthy that this is a rather rare example of the use of a tertiary amine methacrylate monomer to generate the core-forming block during PISA. In this context, the only other literature example of which we are aware utilized 2-(diisopropylamino)ethyl methacrylate.[65]

The RAFT dispersion polymerization of DMA in D5 silicone oil exhibited similar kinetics to previously reported PISA formulations conducted in non-polar solvents. Initially, the relatively slow solution polymerization of DMA was observed. Once a critical degree of polymerization was obtained for the growing PDMA block, micellar nucleation occurred - as indicated by the onset of turbidity in the reaction solution and confirmed by TEM studies. Thereafter, the polymerization became heterogeneous and proceeded within monomer-swollen nascent nanoparticles. This relatively high local DMA concentration led to a three-fold rate enhancement, which enabled 87 % conversion to be achieved within 4 h at 90 °C. GPC analysis confirmed a linear evolution of M_n with conversion while dispersities remained below 1.40 throughout the polymerization, as expected for a reasonably well-controlled RAFT polymerization.

A phase diagram was constructed to enable the reproducible targeting of pure spheres, worms or vesicles. Samples of pure worms formed free-standing gels at room temperature, which is consistent with

the behavior of concentrated dispersions of worm-like micelles reported in the literature. The worm gels formed by $PDMS_{66}$-$PDMA_{105}$ were characterized via oscillatory rheology. Such gels have a G' of 1057 Pa at 30 % w/w and a relatively high critical gelation concentration of approximately 10 – 12 % w/w. Furthermore, synchrotron SAXS was utilized to characterize selected examples of spheres, worms and vesicles in dilute solution. Fitting the scattering patterns to appropriate models enabled calculation of the volume-average sphere core radius, the worm cross sectional radius, the overall vesicle diameter and the mean vesicle membrane thickness. Unfortunately, the worm contour length (estimated to exceed 1.5 μm on the basis of TEM images) could not be reliably determined because the instrument resolution was insufficient at low q. Finally, the mean aggregation numbers for $PDMS_{66}$-$PDMA_{49}$ spheres and $PDMS_{66}$-$PDMA_{191}$ vesicles were determined to be 196 and 48,337, respectively.

In addition to D5 silicone oil, $PDMS_{66}$-$PDMA_{91-105}$ worms were also prepared in HMDS, *n*-dodecane or D4. Such worms can increase the solution viscosity by a factor of up to sixty at copolymer concentrations as low as 5.0 % w/w. Hence, these new PISA formulations offer potential applications as viscosity modifiers for non-polar media in general and silicone oils in particular.

Supporting Information

The Supporting Information is available free of charge on the ACS Publications website at DOI:

GPC traces for $PDMS_{66}$ macro-CTA, Beer-Lambert calibration curve for PETTC, GPC data for kinetics experiment, summary of copolymer characterization data for phase diagram, additional TEM images, tabulated SAXS data, further GPC data and details of SAXS models.

Svetomir Tzokov at the University of Sheffield Biomedical Science Electron Microscopy suite. We also thank the three reviewers of this manuscript for their helpful comments.

Notes

References

(1)   Krause, S. Dilute Solution Properties of a Styrene—Methyl Methacrylate Block Copolymer. *J. Phys. Chem.* **1964**, *68*, 1948–1955.

(2)   Tuzar, Z.; Kratochvíl, P. Block and Graft Copolymer Micelles in Solution. *Adv. Colloid Interface Sci.* **1976**, *6*, 201–232.

(3)   Israelachvili, J. N.; Mitchell, D. J.; Ninham, B. W. Theory of Self-Assembly of Hydrocarbon Amphiphiles into Micelles and Bilayers. *J. Chem. Soc. Faraday Trans. 2* **1976**, *72*, 1525–1568.

(4)   Won, Y.-Y.; Davis, H. T.; Bates, F. S. Giant Wormlike Rubber Micelles. *Science* **1999**, *283*, 960–963.

(5)   Zhang, L.; Eisenberg, A. Multiple Morphologies of "Crew-Cut" Aggregates of Polystyrene-B-Poly(acrylic Acid) Block Copolymers. *Science* **1995**, *268*, 1728–1731.

(6)   Zhang, L.; Eisenberg, A. Multiple Morphologies and Characteristics of "Crew-Cut" Micelle-like Aggregates of Polystyrene-B-Poly(acrylic Acid) Diblock Copolymers in Aqueous Solutions. *J. Am. Chem. Soc.* **1996**, *118*, 3168–3181.

(7)   Antonietti, M.; Förster, S. Vesicles and Liposomes: A Self-Assembly Principle Beyond Lipids. *Adv. Mater.* **2003**, *15*, 1323–1333.

(8)   Discher, D. E.; Eisenberg, A. Polymer Vesicles. *Science* **2002**, *297*, 967–973.

(9)   Dalhaimer, P.; Engler, A. J.; Parthasarathy, R.; Discher, D. E. Targeted Worm Micelles. *Biomacromolecules* **2004**, *5*, 1714–1719.

(10)   Jain, S.; Bates, F. S. On the Origins of Morphological Complexity in Block Copolymer Surfactants. *Science* **2003**, *300*, 460–464.

(11)   Xu, R.; Winnik, M. A.; Hallett, F. R.; Riess, G.; Croucher, M. D. Light-Scattering Study of the Association Behavior of Styrene-Ethylene Oxide Block Copolymers in Aqueous Solution. *Macromolecules* **1991**, *24*, 87–93.

(12)   Charleux, B.; Delaittre, G.; Rieger, J.; D'Agosto, F. Polymerization-Induced Self-Assembly: From Soluble Macromolecules to Block Copolymer Nano-Objects in One Step. *Macromolecules* **2012**, *45*, 6753–6765.

(13)   Canning, S. L.; Smith, G. N.; Armes, S. P. A Critical Appraisal of RAFT-Mediated Polymerization-Induced Self-Assembly. *Macromolecules* **2016**, *49*, 1985–2001.

(14)   Derry, M. J.; Fielding, L. A.; Armes, S. P. Polymerization-Induced Self-Assembly of Block Copolymer Nanoparticles via RAFT Non-Aqueous Dispersion Polymerization. *Prog. Polym. Sci.* **2016**, *52*, 1–18.

(15)   Warren, N. J.; Armes, S. P. Polymerization-Induced Self-Assembly of Block Copolymer Nano-Objects via RAFT Aqueous Dispersion Polymerization. *J. Am. Chem. Soc.* **2014**, *136*, 10174–10185.

(16)   Moad, G.; Rizzardo, E.; Thang, S. H. Living Radical Polymerization by the RAFT Process. *Aust. J. Chem.* **2005**, *58*, 379–410.

(17)   Chiefari, J.; Chong, Y. K. B.; Ercole, F.; Krstina, J.; Jeffery, J.; Le, T. P. T.; Mayadunne, R. T. A.; Meijs, G. F.; Moad, C. L.; Moad, G.; et al. Living Free-Radical Polymerization by Reversible Addition−Fragmentation Chain Transfer: The RAFT Process. *Macromolecules* **1998**, *31*, 5559–

5562.

(18)   Keddie, D. J. A Guide to the Synthesis of Block Copolymers Using Reversible-Addition Fragmentation Chain Transfer (RAFT) Polymerization. *Chem. Soc. Rev.* **2014**, *43*, 496–505.

(19)   Perrier, S. 50th Anniversary Perspective: RAFT Polymerization - A User Guide. *Macromolecules* **2017**, *50*, 7433–7447.

(20)   Derry, M. J.; Fielding, L. A.; Armes, S. P. Industrially-Relevant Polymerization-Induced Self-Assembly Formulations in Non-Polar Solvents: RAFT Dispersion Polymerization of Benzyl Methacrylate. *Polym. Chem.* **2015**, *6*, 3054–3062.

(21)   Lopez-Oliva, A. P.; Warren, N. J.; Rajkumar, A.; Mykhaylyk, O. O.; Derry, M. J.; Doncom, K. E. B.; Rymaruk, M. J.; Armes, S. P. Polydimethylsiloxane-Based Diblock Copolymer Nano-Objects Prepared in Nonpolar Media via RAFT-Mediated Polymerization-Induced Self-Assembly. *Macromolecules* **2015**, *48*, 3547–3555.

(22)   Grazon, C.; Rieger, J.; Sanson, N.; Charleux, B. Study of poly(N,N-Diethylacrylamide) Nanogel Formation by Aqueous Dispersion Polymerization of N,N-Diethylacrylamide in the Presence of Poly(ethylene Oxide)-B-poly(N,N-Dimethylacrylamide) Amphiphilic Macromolecular RAFT Agents. *Soft Matter* **2011**, *7*, 3482–3490.

(23)   Boissé, S.; Rieger, J.; Belal, K.; Di-Cicco, A.; Beaunier, P.; Li, M.-H.; Charleux, B. Amphiphilic Block Copolymer Nano-Fibers via RAFT-Mediated Polymerization in Aqueous Dispersed System. *Chem. Commun.* **2010**, *46*, 1950–1952.

(24)   Zhang, X.; Boissé, S.; Zhang, W.; Beaunier, P.; D'Agosto, F.; Rieger, J.; Charleux, B. Well-Defined Amphiphilic Block Copolymers and Nano-Objects Formed in Situ via RAFT-Mediated Aqueous Emulsion Polymerization. *Macromolecules* **2011**, *44*, 4149–4158.

(25)   Warren, N. J.; Mykhaylyk, O. O.; Mahmood, D.; Ryan, A. J.; Armes, S. P. RAFT Aqueous

Dispersion Polymerization Yields Poly(ethylene Glycol)-Based Diblock Copolymer Nano-Objects with Predictable Single Phase Morphologies. *J. Am. Chem. Soc.* **2014**, *136*, 1023–1033.

(26) Cunningham, V. J.; Alswieleh, A. M.; Thompson, K. L.; Williams, M.; Leggett, G. J.; Armes, S. P.; Musa, O. M. Poly(glycerol monomethacrylate)–Poly(benzyl Methacrylate) Diblock Copolymer Nanoparticles via RAFT Emulsion Polymerization: Synthesis, Characterization, and Interfacial Activity. *Macromolecules* **2014**, *47*, 5613–5623.

(27) Rymaruk, M. J.; Thompson, K. L.; Derry, M. J.; Warren, N. J.; Ratcliffe, L. P. D.; Williams, C. N.; Brown, S. L.; Armes, S. P. Bespoke Contrast-Matched Diblock Copolymer Nanoparticles Enable the Rational Design of Highly Transparent Pickering Double Emulsions. *Nanoscale* **2016**, *8*, 14497–14506.

(28) Sun, J.-T.; Hong, C.-Y.; Pan, C.-Y. Recent Advances in RAFT Dispersion Polymerization for Preparation of Block Copolymer Aggregates. *Polym. Chem.* **2013**, 873–881.

(29) Wan, W.-M.; Hong, C.-Y.; Pan, C.-Y. One-Pot Synthesis of Nanomaterials via RAFT Polymerization Induced Self-Assembly and Morphology Transition. *Chem. Commun.* **2009**, No. 39, 5883–5885.

(30) Wan, W.-M.; Pan, C.-Y. One-Pot Synthesis of Polymeric Nanomaterials via RAFT Dispersion Polymerization Induced Self-Assembly and Re-Organization. *Polym. Chem.* **2010**, *1*, 1475–1484.

(31) Semsarilar, M.; Jones, E. R.; Blanazs, A.; Armes, S. P. Efficient Synthesis of Sterically-Stabilized Nano-Objects via RAFT Dispersion Polymerization of Benzyl Methacrylate in Alcoholic Media. *Adv. Mater.* **2012**, *24*, 3378–3382.

(32) Wan, W.-M.; Sun, X.-L.; Pan, C.-Y. Morphology Transition in RAFT Polymerization for Formation of Vesicular Morphologies in One Pot. *Macromolecules* **2009**, *42*, 4950–4952.

(33) Pei, Y.; Dharsana, N. C.; van Hensbergen, J. A.; Burford, R. P.; Roth, P. J.; Lowe, A. B. RAFT

Dispersion Polymerization of 3-Phenylpropyl Methacrylate with poly[2-(Dimethylamino)ethyl Methacrylate] Macro-CTAs in Ethanol and Associated Thermoreversible Polymorphism. *Soft Matter* **2014**, *10*, 5787–5796.

(34) Zhang, Q.; Zhu, S. Ionic Liquids: Versatile Media for Preparation of Vesicles from Polymerization-Induced Self-Assembly. *ACS Macro Lett.* **2015**, *4*, 755–758.

(35) Kang, Y.; Pitto-Barry, A.; Willcock, H.; Quan, W.-D.; Kirby, N.; Sanchez, A. M.; O'Reilly, R. K. Exploiting Nucleobase-Containing Materials – from Monomers to Complex Morphologies Using RAFT Dispersion Polymerization. *Polym. Chem.* **2015**, *6*, 106–117.

(36) Kang, Y.; Pitto-Barry, A.; Maitland, A.; O'Reilly, R. K. RAFT Dispersion Polymerization: A Method to Tune the Morphology of Thymine-Containing Self-Assemblies. *Polym. Chem.* **2015**, *6*, 4984–4992.

(37) Pei, Y.; Sugita, O. R.; Thurairajah, L.; Lowe, A. B. Synthesis of Poly(stearyl Methacrylate-B-3-Phenylpropyl Methacrylate) Nanoparticles in N-Octane and Associated Thermoreversible Polymorphism. *RSC Adv.* **2015**, *5*, 17636–17646.

(38) Fielding, L. A.; Derry, M. J.; Ladmiral, V.; Rosselgong, J.; Rodrigues, A. M.; Ratcliffe, L. P. D.; Sugihara, S.; Armes, S. P. RAFT Dispersion Polymerization in Non-Polar Solvents: Facile Production of Block Copolymer Spheres, Worms and Vesicles in N-Alkanes. *Chem. Sci.* **2013**, *4*, 2081–2087.

(39) Zong, M.; Thurecht, K. J.; Howdle, S. M. Dispersion Polymerisation in Supercritical CO2 Using Macro-RAFT Agents. *Chem. Commun.* **2008**, *45*, 5942.

(40) Thurecht, K. J.; Gregory, A. M.; Wang, W.; Howdle, S. M. "Living" polymer Beads in Supercritical CO2. *Macromolecules* **2007**, *40*, 2965–2967.

(41) Mata, A.; Fleischman, A. J.; Roy, S. Characterization of Polydimethylsiloxane (PDMS) Properties

for Biomedical Micro/nanosystems. *Biomed. Microdevices* **2005**, *7*, 281–293.

(42) Bergeron, V.; Cooper, P.; Fischer, C.; Giermanska-Kahn, J.; Langevin, D.; Pouchelon, A. Polydimethylsiloxane (PDMS)-Based Antifoams. *Colloids Surfaces A Physicochem. Eng. Asp.* **1997**, *122*, 103–120.

(43) Jakobsen, J.; Sanborn, D. M.; Winer, W. O. Pressure Viscosity Characteristics of a Series of Siloxane Fluids. *J. Lubr. Technol.* **1974**, *96*, 410–417.

(44) Horii, Y.; Kannan, K. Survey of Organosilicone Compounds, Including Cyclic and Linear Siloxanes, in Personal-Care and Household Products. *Arch. Environ. Contam. Toxicol.* **2008**, *55*, 701–710.

(45) Wang, R.; Moody, R. P.; Koniecki, D.; Zhu, J. Low Molecular Weight Cyclic Volatile Methylsiloxanes in Cosmetic Products Sold in Canada: Implication for Dermal Exposure. *Environ. Int.* **2009**, *35*, 900–904.

(46) Semsarilar, M.; Ladmiral, V.; Blanazs, A.; Armes, S. P. Anionic Polyelectrolyte-Stabilized Nanoparticles via RAFT Aqueous Dispersion Polymerization. *Langmuir* **2012**, *28*, 914–922.

(47) Couvreur, L.; Lefay, C.; Belleney, J.; Charleux, B.; Guerret, O.; Magnet, S. First Nitroxide-Mediated Controlled Free-Radical Polymerization of Acrylic Acid. *Macromolecules* **2003**, *36*, 8260–8267.

(48) Trent, J. S.; Scheinbeim, J. I.; Couchman, P. R. Ruthenium Tetraoxide Staining of Polymers for Electron Microscopy. *Macromolecules* **1983**, *16*, 589–598.

(49) Pal, S.; Ghosh Roy, S.; De, P. Synthesis via RAFT Polymerization of Thermo- and pH-Responsive Random Copolymers Containing Cholic Acid Moieties and Their Self-Assembly in Water. *Polym. Chem.* **2014**, *5*, 1275–1284.

(50)   Zhang, X.; Rieger, J.; Charleux, B. Effect of the Solvent Composition on the Morphology of Nano-Objects Synthesized via RAFT Polymerization of Benzyl Methacrylate in Dispersed Systems. *Polym. Chem.* **2012**, *3*, 1502–1509.

(51)   Rieger, J.; Stoffelbach, F.; Bui, C.; Alaimo, D.; Jérôme, C.; Charleux, B. Amphiphilic Poly(ethylene Oxide) Macromolecular RAFT Agent as a Stabilizer and Control Agent in Ab Initio Batch Emulsion Polymerization. *Macromolecules* **2008**, *41*, 4065–4068.

(52)   Blanazs, A.; Ryan, A. J.; Armes, S. P. Predictive Phase Diagrams for RAFT Aqueous Dispersion Polymerization: Effect of Block Copolymer Composition, Molecular Weight, and Copolymer Concentration. *Macromolecules* **2012**, *45*, 5099–5107.

(53)   Tan, J.; Sun, H.; Yu, M.; Sumerlin, B. S.; Zhang, L. Photo-PISA: Shedding Light on Polymerization-Induced Self-Assembly. *ACS Macro Lett.* **2015**, *4*, 1249–1253.

(54)   Figg, C. A.; Simula, A.; Gebre, K. A.; Tucker, B. S.; Haddleton, D. M.; Sumerlin, B. S. Polymerization-Induced Thermal Self-Assembly (PITSA). *Chem. Sci.* **2015**, *6*, 1230–1236.

(55)   Blanazs, A.; Madsen, J.; Battaglia, G.; Ryan, A. J.; Armes, S. P. Mechanistic Insights for Block Copolymer Morphologies: How Do Worms Form Vesicles? *J. Am. Chem. Soc.* **2011**, *133*, 16581–16587.

(56)   Jones, E. R.; Semsarilar, M.; Blanazs, A.; Armes, S. P. Efficient Synthesis of Amine-Functional Diblock Copolymer Nanoparticles via RAFT Dispersion Polymerization of Benzyl Methacrylate in Alcoholic Media. *Macromolecules* **2012**, *45*, 5091–5098.

(57)   Zhou, W.; Qu, Q.; Xu, Y.; An, Z. Aqueous Polymerization-Induced Self-Assembly for the Synthesis of Ketone-Functionalized Nano-Objects with Low Polydispersity. *ACS Macro Lett.* **2015**, *4*, 495–499.

(58)   Cunningham, V. J.; Ning, Y.; Armes, S. P.; Musa, O. M. Poly(N -2-(Methacryloyloxy)ethyl

Pyrrolidone)-Poly(benzyl Methacrylate) Diblock Copolymer Nano-Objects via RAFT Alcoholic Dispersion Polymerisation in Ethanol. *Polymer* **2016**, *106*, 189–199.

(59) Jones, E. R.; Semsarilar, M.; Wyman, P.; Boerakker, M.; Armes, S. P. Addition of Water to an Alcoholic RAFT PISA Formulation Leads to Faster Kinetics but Limits the Evolution of Copolymer Morphology. *Polym. Chem.* **2016**, *7*, 851–859.

(60) Jesson, C. P.; Cunningham, V. J.; Smallridge, M. J.; Armes, S. P. Synthesis of High Molecular Weight Poly(glycerol Monomethacrylate) via RAFT Emulsion Polymerization of Isopropylideneglycerol Methacrylate. *Macromolecules* **2018**, *51*, 3221–3232.

(61) Derry, M. J.; Fielding, L. A.; Warren, N. J.; Mable, C. J.; Smith, A. J.; Mykhaylyk, O. O.; Armes, S. P. In Situ Small-Angle X-Ray Scattering Studies of Sterically-Stabilized Diblock Copolymer Nanoparticles Formed during Polymerization-Induced Self-Assembly in Non-Polar Media. *Chem. Sci.* **2016**, *7*, 5078–5090.

(62) Fielding, L. A.; Lane, J. A.; Derry, M. J.; Mykhaylyk, O. O.; Armes, S. P. Thermo-Responsive Diblock Copolymer Worm Gels in Non-Polar Solvents. *J. Am. Chem. Soc.* **2014**, *136*, 5790–5798.

(63) Dzuy, N. Q.; Boger, D. V. Yield Stress Measurement for Concentrated Suspensions. *J. Rheol.* **1983**, *27*, 321–349.

(64) Penfold, N. J. W.; Lovett, J. R.; Verstraete, P.; Smets, J.; Armes, S. P. Stimulus-Responsive Non-Ionic Diblock Copolymers: Protonation of a Tertiary Amine End-Group Induces Vesicle-to-Worm or Vesicle-to-Sphere Transitions. *Polym. Chem.* **2017**, *8*, 272–282.

(65) Mable, C. J.; Fielding, L. A.; Derry, M. J.; Mykhaylyk, O. O.; Chambon, P.; Armes, S. P. Synthesis and pH-Responsive Dissociation of Framboidal ABC Triblock Copolymer Vesicles in Aqueous Solution. *Chem. Sci.* **2018**, *9*, 1454–1463.